PHYSICAL REVIEW E **92**, 031301(R) (2015)

Liquid nanodroplet formation through phase explosion mechanism in laser-irradiated metal targets

Alberto Mazzi,[1,*] Federico Gorrini,[1,2] and Antonio Miotello[1]

[1]*Dipartimento di Fisica, Università degli Studi di Trento, 38123 Povo (Trento), Italy*

[2]*Center for Neuroscience and Cognitive Systems @UniTn, Istituto Italiano di Tecnologia, Corso Bettini 31, 38068 Rovereto, Italy*

(Received 23 June 2015; published 21 September 2015)

Some quantitative aspects of laser-irradiated pure metals, while approaching phase explosion, are still not completely understood. Here, we develop a model that describes the main quantities regulating the liquid-vapor explosive phase transition and the expulsion of liquid nanodroplets that, by solidifying, give rise to nanoparticle formation. The model combines both a thermodynamics description of the explosive phase change and a Monte Carlo simulation of the randomly generated critical vapor bubbles. The calculation is performed on a set of seven metals (Al, Fe, Co, Ni, Cu, Ag, and Au) which are frequently used in pulsed laser ablation experiments. Our final predictions about the size distribution of the liquid nanodroplets and the number ratio of liquid/vapor ejected atoms are compared, whenever possible, with available molecular dynamics simulations and experimental data.

DOI: 10.1103/PhysRevE.92.031301 PACS number(s): 02.70.−c, 79.20.Eb, 47.55.db, 64.70.F−

Introduction. Phase explosion was found to be the most efficient mechanism in the pulsed laser ablation of metals when looking at thermal processes for sufficiently short time scales (in the nanosecond to femtosecond range) [1]. This phenomenon is predicted to occur in metastable liquids at temperatures of about 90% of the thermodynamic critical temperature T_c [2], when a so dense distribution of vapor bubbles is generated through homogeneous nucleation that the liquid phase is broken into a mixture of vapor and small scale liquid droplets, leaving the target [3].

In the modeling of phase explosion conditions, continuum approaches based on thermodynamics are led to the limits of their validity. On the other hand, continuum models are very handy and accessible [4], and it is worthwhile to compare their predictions and extrapolations with the results coming from experiments and atomistic simulations.

The present Rapid Communication aims to model the phase explosion process in a metal target through a continuum approach. The starting point of our study is the description of the thermodynamic properties of metastable liquid metals up to temperatures close to T_c. Then the theory of homogeneous nucleation is briefly considered, with the goal of designing a three-dimensional (3D) Monte Carlo (MC) simulation of homogeneous nucleation. In particular, we will use the known nucleation theory to evaluate the critical radius r_c of vapor bubbles, generated in the phase explosion and to be used in the simulation. The MC simulation aims to generate a dense and connected distribution of supercritical vapor bubbles which causes the breaking of the liquid phase, giving rise to a distribution of liquid nanodroplets and vapor atoms. The solidification of liquid nanodroplets, during flight from the target to substrate, and also on substrate, generates nanoparticles (NPs) if ablation occurs in vacuum conditions. In the presence of an external atmosphere, other mechanisms are present, especially collisional cooling leading to the condensation of expelled atoms. The liquid versus vapor composition of the bulk material in phase explosion conditions as well as the size distribution of the expelled liquid nanodroplets are calculated. Our results, regarding a set of seven metals (Al, Fe, Co, Ni, Cu, Ag, and Au) commonly used as pure targets in laser ablation experiments, are compared with the available literature data, both regarding experimental data and molecular dynamics simulations. While designing the MC simulation we focused it on the nanosecond irradiation regime in order to be able to make some simplifying assumptions.

Thermodynamic properties of metastable liquid metals. Since our study aims to describe liquid nanodroplet expulsion from laser-irradiated targets leading to nanoparticle production in the phase explosion process, we are particularly interested in those models which relate the thermodynamic critical point to surface tension, which is the fundamental quantity which allows us to describe the homogeneous nucleation of vapor bubbles in the superheated liquid.

Quite recently, Blairs *et al.* [5] derived a method to calculate T_c using surface tension and liquid density values at the melting point T_m. The approach is based on the Lennard-Jones potential for liquid metals. Their study is based on the experimental fitting of semiempirical laws with data regarding 18 different metals. As a result, their work provides an equation to predict T_c for pure metals, looking at the experimental measurements of surface tension and molar volume (σ_m and v_m) both given at T_m,

$$T_c = \sigma_m \left(\frac{v_m m}{(C v_m)^{5/6} - q} \right)^4, \tag{1}$$

where $m = 8.9733 \times 10^{-19}$, $q = -1.0459 \times 10^{-25}$, and $C = 1.484 \pm 0.025$ are empirical fit parameters. In Table I we show the estimations of T_c for the metallic elements examined in our study. Details about the data for σ_m and v_m are given in Table II.

While studying the liquid-vapor phase transition of a pure substance, the fundamental thermodynamic quantities describing the two coexisting phases (temperature, saturated vapor pressure p_s and vapor and liquid molar volumes v_v and v_l) obey to the Clausius-Clapeyron equation,

$$\frac{dp_s}{dT} = \frac{\Delta h_v(T)}{T[v_v(T) - v_l(T)]}, \tag{2}$$

where Δh_v is the molar enthalpy of vaporization. In the present study we will consider semiempirical models for the functions

*alberto.mazzi-1@unitn.it

TABLE I. Critical parameters estimated in this work.

Metal	T_c (K)	ρ_c(kg/m^3)	P_c (10^8 Pa)
Al	6319	634	3.2
Fe	8059	1467	5.4
Co	7710	1350	5.4
Ni	7241	2159	6.5
Cu	5741	2363	4.6
Ag	5851	2718	3.3
Au	7003	5066	3.9

$\Delta h_v(T)$, $v_v(T)$, and $v_l(T)$ and we will integrate the Clausius-Clapeyron differential equation to compute $p_s(T)$, similarly to the approach proposed by Hornung [9].

According to theoretical and computational studies, together with experimental observations [10–13], the liquid and vapor densities ρ_l and ρ_v at phase coexistence can be modeled as two power series, with universal exponents and four material-dependent coefficients,

$$\begin{aligned}\frac{\rho_l(T)}{\rho_c} &= 1 + D_0\Delta T + C_1(\Delta T)^{\beta_c} \\ &\quad + D_1(\Delta T)^{1-\alpha} + C_2(\Delta T)^{\beta_c+\Delta}, \\ \frac{\rho_v(T)}{\rho_c} &= 1 + D_0\Delta T - C_1(\Delta T)^{\beta_c} \\ &\quad + D_1(\Delta T)^{1-\alpha} - C_2(\Delta T)^{\beta_c+\Delta}, \end{aligned} \tag{3}$$

where $\Delta T = \frac{T_c - T}{T_c}$, $\alpha \approx 0.109$, $\beta_c = 0.325$, and $\Delta = 0.51$. Equation (3), independently from the choice of the coefficients, is consistent with the fact that the densities of both the phases tend to the critical density ρ_c at the critical point.

In the present work we give estimations of ρ_c and of the coefficients D_0, D_1, C_1, and C_2, obtained through a least square fit of Eq. (3) with available experimental data for ρ_l in the range $T_m < T < T_b$, where T_m and T_b are the temperatures at the melting point and at the normal boiling point. Near T_b we assume an ideal gas behavior, which provides $\rho_v(T_b) = \frac{mP_{\text{atm}}}{k_B T}$ and $\frac{d\rho_v}{dT}(T_b) = \frac{mP_{\text{atm}}}{k_B T}\frac{\frac{\Delta h_v}{RT_b}-1}{T_b}$. Final results are reported in Table III.

The predicted coexistence curve, shown in Fig. 1(a), is similar to the results of recent papers [12,13].

Concerning the enthalpy of vaporization, we refer to the well known formula proposed by Watson in 1943 [18] which

TABLE III. Results of the density interpolations. In the first column, the references for the experimental measurements of the liquid density used in the calculation.

Metal	ρ_c(kg/m^3)	D_0	C_1	D_1	C_2
Al [14]	634 ± 5	1.1 ± 0.2	1.75 ± 0.04	-0.17	0.08
Fe [15]	1467 ± 53	1.8 ± 0.5	1.51 ± 0.08	-0.24	1.02
Co [6,16][a]	≈ 1350	≈ 3.1	≈ 1.3	-0.70	2.01
Ni [15]	2159 ± 45	1.1 ± 0.3	1.75 ± 0.04	-0.15	0.10
Cu [14]	2363 ± 23	1.2 ± 0.2	1.82 ± 0.03	-0.27	-0.02
Ag [6,17]	2718 ± 55	1.4 ± 0.3	1.68 ± 0.04	-0.57	0.06
Au [17]	5066 ± 5	1.4 ± 0.1	1.73 ± 0.01	-0.64	-0.07

[a]Poor knowledge of liquid density.

can be applied to the entire liquid range from T_m to T_c:

$$\Delta h_v(T) = \Delta h_{v0}\left(\frac{\Delta T}{\Delta T_0}\right)^{0.38}. \tag{4}$$

It is an empirical law, where T_0 and Δh_{v0} are data generally associated with the normal boiling point, say, T_b and $\Delta h_v(T_b)$. Equation (4) was proved to be a reliable estimation for many organic and inorganic pure substances [19] and also for transition metals [20].

Finally, for the temperature dependence of surface tension, we employ the empirical formula proposed in 1945 by Guggenheim [21],

$$\sigma(T) = \sigma_0\left(1 - \frac{T}{T_c}\right)^{\frac{11}{9}} = \sigma_m\left(\frac{\Delta T}{\Delta T_m}\right)^{\frac{11}{9}}, \tag{5}$$

with $\Delta T_m = \frac{T_c - T_m}{T_c}$. This formula is still well considered, and has been applied to various chemical compounds [19] and recently also to metallic elements [22].

Homogeneous nucleation modeling. Here we will briefly look at the theory of homogeneous nucleation of vapor bubbles in a metastable liquid in order to estimate the typical values of the critical radius r_c of vapor bubbles, which is the only physical parameter to be given as an input to our computational simulation. At the end of this analysis we fix the time duration of the phase explosion (precisely defined below) at $\tau_{\text{pe}} = 1$ ns. This choice, operated in the framework of the nucleation theory, will allow us to consistently calculate the thermodynamic and kinetic quantities to characterize the phase explosion and, furthermore, to estimate the critical radius as required by the MC method.

TABLE II. Parameters used for the thermodynamic modeling with corresponding references: Molar mass M, melting temperature T_m, boiling temperature T_b, liquid density at the melting point ρ_m, surface tension at the melting point σ_m, and enthalpy of vaporization at the boiling point $\Delta h_v(T_b)$.

Metal	M (g/mol) [6]	T_m (K) [6]	T_b (K) [6]	ρ_m(kg/m^3) [6]	σ_m (N/m) [7]	$\Delta h_v(T_b)$ (kJ/mol)
Al	26.982	933	2792	2375	1.05	294 [6]
Fe	55.845	1811	3134	6980	1.909	355 [8]
Co	58.933	1768	3200	7750	1.928	375 [8]
Ni	58.693	1728	3186	7810	1.834	378 [8]
Cu	63.546	1358	2835	8020	1.374	300 [8]
Ag	107.868	1235	2435	9320	0.955	255 [8]
Au	196.867	1337	3129	17 310	1.162	324 [6]

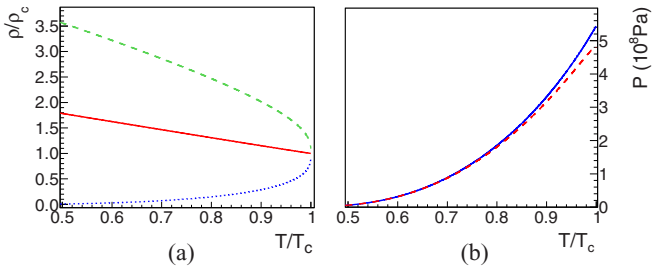

FIG. 1. (Color online) (a) Coexistence curve. ρ_l/ρ_c (dashed green curve), ρ_v/ρ_c (dotted blue), and average density (solid red). (b) Saturated pressure (solid blue) and vapor pressure (dashed red), calculated for iron.

The appearance of a gas bubble in a bulk liquid phase is microscopically determined by the presence of a vaporlike density fluctuation staying in labile thermodynamic equilibrium with the liquid [23] (homogeneous nucleation). This fluctuation will generate a critical nucleus if, by acquiring even a single additional molecule, it starts growing spontaneously.

In classical nucleation theory, assuming the liquid to be incompressible and the vapor to behave ideally, the vapor pressure inside critical spherical nuclei (p_v) is given by [24]

$$p_v = p_s \exp\left[(p_l - p_s)\frac{v_l}{k_B T}\right], \tag{6}$$

where p_l and v_l are the pressure and the molar volume of the liquid phase, respectively. Since the saturated vapor pressure can be obtained through integration of the Clausius-Clapeyron equation (2), we only need an estimation of p_l in order to calculate p_v from Eq. (6). In the case of pulsed laser ablation of metals in vacuum, p_l is determined by the pressure exerted on the molten target surface by the vaporized material. To our purpose we can consider the surface temperature T_s to be of the order of $0.90T_c$ and the environment gas pressure negligible compared to the saturated vapor pressure $p_s(T_s)$. An idealized solution was proposed by Anisimov [25] and further developed by Knight [26], with the final outcome $p_l = 0.55 p_s(T_s)$. This means that, under pulsed laser ablation of metals in vacuum, the metastable liquid reaches pressures of the order of 10^8 Pa due to the recoil pressure.

The radius of the critical nuclei can be described by

$$r_c = \frac{2\sigma}{p_v - p_l}. \tag{7}$$

The nucleation of such critical nuclei requires one to overcome the energy barrier given by the free energy of formation W_c, for which we can obtain the following Gibbs classical expression:

$$W_c = \frac{4}{3}\pi r_c^2 \sigma = \frac{16\pi\sigma^3}{3(p_v - p_l)^2}. \tag{8}$$

Finally, the nucleation rate J_s of near-critical vapor nuclei per unit volume in the case of a steady nucleation process can be expressed, owing to a theoretical result obtained by Döring [27] and Volmer [28], in the form reported by Skripov [29],

$$J_s = n_l \sqrt{\frac{6\sigma}{(3-b)\pi m}} e^{-\frac{\Delta h_v}{RT}} e^{-\frac{W_c}{k_B T}}, \tag{9}$$

where $b = 1 - \frac{p_l}{p_v}$, Δh_v is the molar enthalpy, R is the gas constant, the factor n_l is the number density for the metastable liquid, and W_c can be obtained from Eq. (8).

In general, the stationary nucleation regime is reached asymptotically, with a characteristic time lag $\tau_{\rm lag}$. The time-dependent nucleation frequency can be written as [30]

$$J(t) = J_s \exp\left(-\frac{\tau_{\rm lag}}{t}\right). \tag{10}$$

An expression for this time lag was reported by Skripov [29] and the explicit result is

$$\tau_{\rm lag} = \sqrt{\frac{2\pi M}{RT}} \frac{4\pi\sigma p_v}{(p_v - p_l)^2}, \tag{11}$$

where M is the molar weight of the substance. We can calculate $\tau_{\rm lag}$ as a function of the temperature by Eqs. (6) and (5): For the investigated metals, $\tau_{\rm lag}$ ranges between 10 and 100 ps for temperatures in the range $[0.90,0.95]T_c$. Now focusing our study to the nanosecond pulse regime, so that $\tau_{\rm lag}$ is negligible compared to the heating time scale, we are allowed to assume stationary nucleation.

By neglecting both spatial gradients and temporal variations of the temperature in the material, we are able to estimate the phase explosion time $\tau_{\rm pe}(T)$ as a function of the temperature, defined as the time interval between the appearance of the first critical vapor bubble and phase explosion, at a given temperature $T_{\rm pe}$, which occurs when the distribution of critical bubbles will saturate the liquid volume. The vapor bubble packing fraction can be expressed by the ratio $\eta = \frac{V_v}{V_{\rm tot}}$ and the maximum packing fraction results to be $\eta_{\rm max} = 0.30$, according to the MC simulation reported below. With these assumptions, $\tau_{\rm pe}(T)$ results to have the following analytic expression,

$$\tau_{\rm pe} = \frac{\alpha}{J_s V_c} \ln\left(1 + \frac{\eta_{\rm max}}{1-\eta_{\rm max}}\frac{1}{\alpha}\right), \tag{12}$$

where $\alpha = \frac{\rho_l}{\rho_v}$ and V_c is the volume of a critical vapor bubble. In the following MC simulation, we chose $\tau_{\rm pe} = 1$ ns, as an indicative example, with a consistent choice of the other quantities, in particular, a constant temperature $T_{\rm pe}$ defined by $\tau_{\rm pe}(T_{\rm pe}) = 1$ ns: Looking at the temperature dependence of J_s in Fig. 2(b), the contribution of nucleation

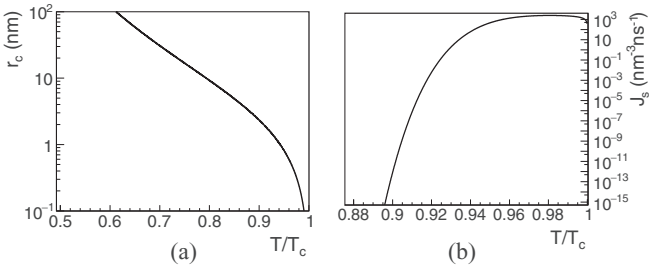

FIG. 2. (a) Critical radius of vapor bubbles in the metastable liquid. (b) Nucleation rate of supercritical bubbles, calculated for iron.

at temperatures lower than that of the stationary regime results to be ineffective, due to the negligible kinetics.

3D Monte Carlo simulation for phase explosion. In our MC simulation we suppose the explosion to occur, according to Ref. [30], when supercritical vapor bubbles, generated in a metastable liquid volume through random homogeneous nucleation, are in contact with each other, forming a kind of percolation cluster in the considered volume. At that moment, liquid nanodroplets and vapor are expelled and we are able to study the final composition of the vapor/liquid mixture and to evaluate the size distribution of the generated nanodroplets leading to nanoparticles.

The critical radius of the vapor bubbles r_c is calculated through Eq. (7) at $T_{\rm pe}$. The observed portion of the target is a 3D cubic volume with size L. If we consider r_c of aluminum at $T_{\rm pe}$ ($r_c = 1.76$ nm), the largest system studied up to now is a cubic box with side $L = 250$ nm, where about 30 000 liquid droplets have been identified.

Our adopted MC method randomly generates N *nucleation sites* (i.e., bubble centers with a first-neighbor distance larger than $2r_c$) with a uniform distribution in order to saturate the available volume. Then, for each site, a bubble radius $r \gtrsim r_c$ is assigned on the base of the algorithm here described. The array of nucleation sites is arranged in ascending order according to the first-neighbor distance so that the radius assignment proceeds with the following rule: If the ith bubble is the first neighbor of its first neighbor with distance d in this random distribution, both of them will have radius $r = d/2$. Otherwise, the first neighbor of the ith bubble, let us say, the jth bubble, has to be already developed, with radius $r_j < d/2$. In this latter case, $r_i = d - r_j$. In this way the bubbles get in touch with their neighbors, with no overlap. A spherical shape is assumed for the nucleated vapor volumes: This is a simplifying assumption, but note that the spherical shape is associated with the minimization of the free energy of the system.

In our case, with a random packing of nonmonodispersed spheres, we obtained a maximum packing fraction of about $\eta_{\rm max} = \frac{V_{\rm bubbles}}{V_{\rm tot}} \approx 0.30$. This value, which represents the intrinsic saturation of our bubble nucleation algorithm, has been taken as a reference for the definition of a dense and connected distribution of supercritical bubbles, as discussed above.

The final step is to study the breaking of the remaining intervolume into liquid nanodroplets. In particular, the remaining liquid phase is still connected, but it is full of vapor bubbles which are in touch with each other along many directions. This 3D problem is rather complex and the adopted algorithm described below is the choice we made after testing different solutions.

In order to separate the intervolumes, a fixed quantity of probe sites is randomly generated in the liquid volume, and for each site the distance from the first liquid-vapor surface is evaluated along 40 directions. Through a weighted average procedure, a radius is associated with each site and the eventual overlapping between adjacent liquid spheres is then evaluated. In this way a distribution of disconnected liquid clusters is identified.

In particular, the 3D adopted algorithm, as described above, when transferred to two dimensions (2D), gives results easily viewable and checkable, as reported in Fig. 3.

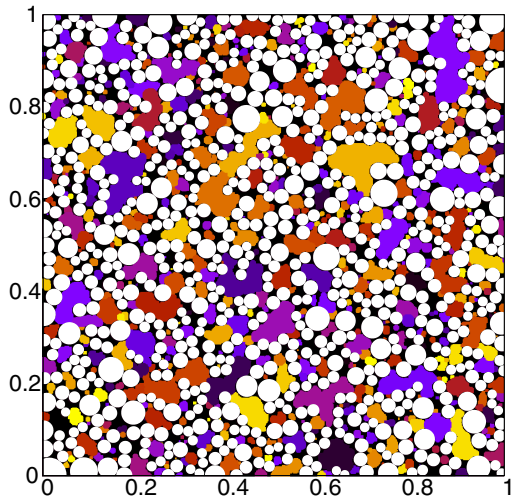

FIG. 3. (Color online) 2D simulation: Supercritical bubbles in white and liquid intervolumes with different colors.

Results and discussion. In Fig. 4(a) we show the resulting bubble and droplet distributions, where the physical parameters of silver have been considered ($r_c = 1.67$ nm). We can compare our result with some recent experimental observation of silver nanoparticles as deposited in vacuum on a substrate and detected by transmission electron microscopy [31] [Fig. 4(b)]. The peak in the diameter distribution observed with our simulation is predicted at about 2.00 nm (1.63 nm if we consider the thermal contraction from $T_{\rm pe}$ to room temperature). The experimental histogram shows a peak diameter of about 5 nm. Some modifications of the distribution are expected due to in-flight interactions and shape arrangement after attachment on the substrate, but the general outcome of this measurement is the observation of a large relative abundance of nanometer-sized particles, in line with our simulation.

A more interesting result can be shown if the volume distribution of the liquid nanodroplets is displayed in a log-log histogram. The 3D liquid droplet size distribution obtained through our algorithm [see Fig. 5(a)] is in good agreement with a power law $f(N) \propto N^{-a}$, where N is the number of atoms per nanodroplet and the exponent a has been estimated as 1.9. The power law has been observed in a quite wide range, between 300 and 10 000 atoms per droplet. Very recently, a molecular dynamics (MD) simulation of an aluminum target irradiated with a 100 fs laser pulse has obtained a detailed result of the size distribution of the ablated atomic clusters [32]. A power law behavior is observed, with different slopes in different size ranges: In particular, in the same range studied by our MC method, the exponent emerging from the MD simulation is $a \approx 1.43$, not much different from ours.

In Table IV we summarize some significant results of our model, in a nanosecond time scale: The estimated temperature ratio for phase explosion, the critical radius calculated at $T_{\rm pe}$, the number of atoms per nanodroplet for peak-size clusters ($r_{\rm peak}$), and the vapor/liquid atomic ratio N_v/N_l which expresses the final relative composition of the ablated material. Here, we can see that for the studied metals, N_v/N_l falls between 30% and 45%. These estimations are

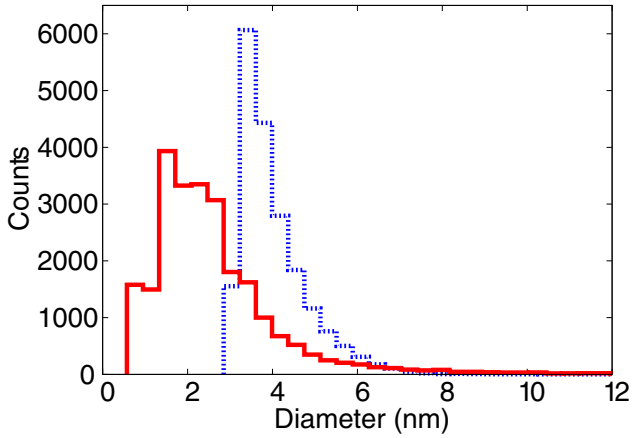

(a)

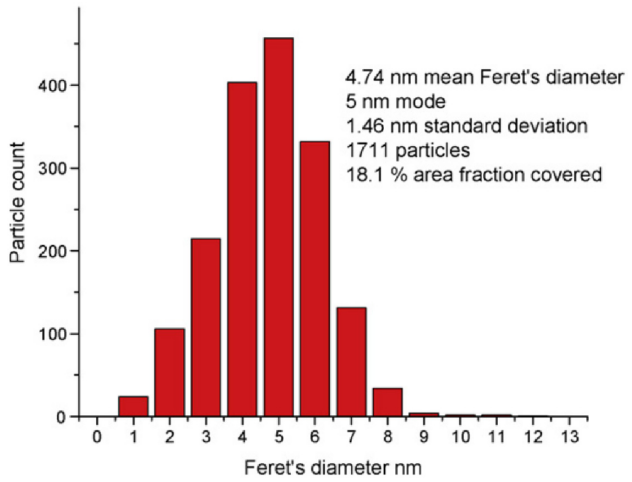

(b)

FIG. 4. (Color online) (a) Diameter distribution for Ag ($r_c = 1.67$ nm): Bubbles in blue (dashed) and droplets in red (solid). (b) Experimental diameter distribution of pure metallic Ag nanoparticles [31].

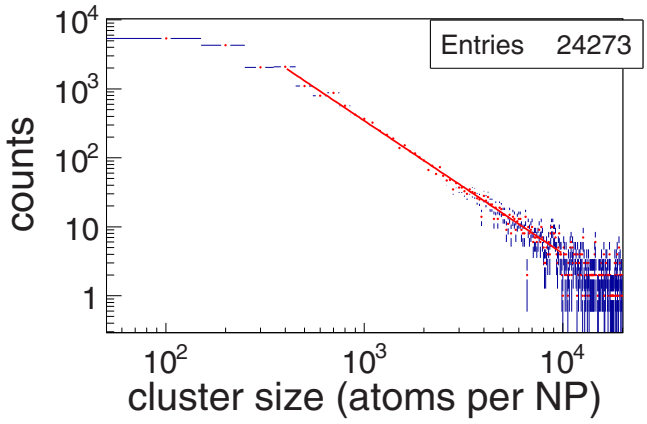

(a)

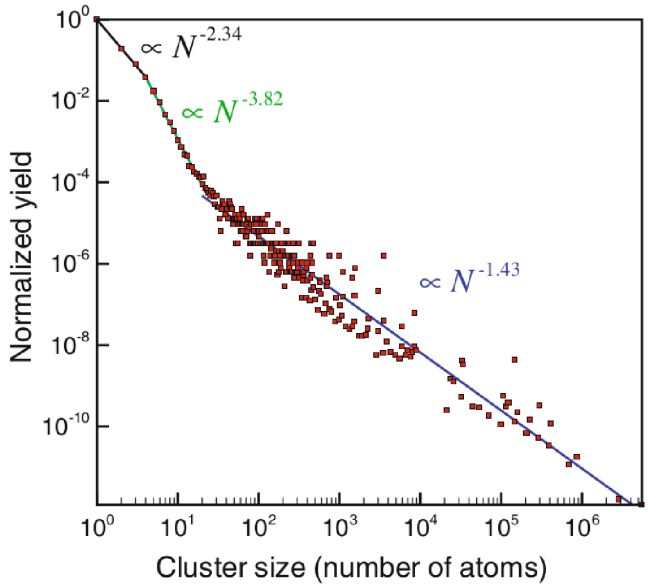

(b)

FIG. 5. (Color online) Volume distribution of the nanodroplets: (a) Our method, liquid Al NPs; (b) MD simulation on Al [32].

in qualitative agreement with experimental measurements: A recent paper [33], which deals with femtosecond laser ablation of copper and gold pure targets in vacuum, reports experimental measurements of the vapor/total number ratio in the ablated plume. The measurement is based on emission intensities integrated over all the plume volumes and were performed at different laser fluences. In particular, at high laser fluences (some J/cm^2) the estimation of $\frac{N_v}{N_{\text{tot}}} \approx \frac{I_{\text{atoms}}}{I_{\text{tot}}}$ is almost constant, with values of about 40% for copper and 8% for gold. These values correspond to $\frac{N_v}{N_l} \approx 0.69$ for copper and $\frac{N_v}{N_l} \approx 0.09$ for gold. It has to be noted that our presented algorithm is specifically designed to give information only about the phase explosion mechanism, while of course the experimental values may be the product of several concurrent phenomena, such as vaporization alone or spallation.

Conclusions. In this study we showed promising results of a thermodynamic modeling of the phase explosion process in metastable liquid metals. We performed our calculations for seven different transition metals, which are frequently used in laser ablation experiments, to show the generality of our results. The phase explosion conditions have been discussed, in particular, focusing on nanosecond pulse regime.

Our model was able to describe many aspects of the liquid nanodroplets directly produced in the external layers of the target through the phase explosion mechanism. In

TABLE IV. Parameters estimated at T_{pe}.

Metal	T_{pe}/T_c	r_c (nm)	N_{atom}/cluster	N_v/N_l
Al	0.91	1.76	145	0.29
Fe	0.92	1.57	114	0.38
Co	0.93	1.54	97	0.41
Ni	0.92	1.42	118	0.33
Cu	0.92	1.49	135	0.31
Ag	0.91	1.67	128	0.32
Au	0.91	1.66	127	0.31

particular, we studied the size distribution of the produced liquid nanodroplets, which give rise to a significant fraction of the ablated material. The size distribution function of nanodroplets was found to fit with a power law in the range between 300 and 10 000 atoms per nanodroplet. Moreover, the experimental observation of nanometer-sized particles in the laser ablation of pure metals can be attributed to the solidification of liquid nanodroplets formed through the phase explosion mechanism.

The present work may be a starting point for future developments. In particular, the description of the nucleation process could be improved by introducing more complicated aspects of the dynamics of vapor bubbles, such as their growth rate and the possibility of bubbles merging at an early stage of nucleation. The simulation may be made more realistic, taking into account a temperature gradient inside the target and a time dependence.

Acknowledgments. We gratefully acknowledge Professor Leonid V. Zhigilei for useful discussions on several topics related to the present work. The computations have been performed on the HPC facility *Wiglaf* at the Physics Department of the University of Trento. The work is partially financially supported by PAT (Provincia Autonoma di Trento) project ENAM in cooperation with Istituto PCB of CNR (Italy).

[1] R. Kelly and A. Miotello, Phys. Rev. E **60**, 2616 (1999).
[2] M. M. Martynyuk, Combust., Explos. Shock Waves **13**, 178 (1977).
[3] R. Kelly and A. Miotello, Appl. Surf. Sci. **96-98**, 205 (1996).
[4] N. M. Bulgakova and A. V. Bulgakov, Appl. Phys. A **73**, 199 (2001).
[5] S. Blairs and M. H. Abbasi, J. Colloid Interface Sci. **304**, 549 (2006).
[6] *CRC Handbook of Chemistry and Physics*, edited by D. R. Lide, 90th ed. (Taylor and Francis, London, 2010).
[7] B. J. Keene, Int. Mater. Rev. **38**, 157 (1993).
[8] H. M. Lu and Q. Jiang, J. Phys. Chem. B **109**, 15463 (2005).
[9] K. Hornung, J. Appl. Phys. **46**, 2548 (1975).
[10] J. Wang and M. A. Anisimov, Phys. Rev. E **75**, 051107 (2007).
[11] S. Jungst, B. Knuth, and F. Hensel, Phys. Rev. Lett. **55**, 2160 (1985).
[12] J. K. Singh, J. Adhikari, and S. K. Kwak, Fluid Phase Equilib. **248**, 1 (2006).
[13] E. M. Apfelbaum, J. Chem. Phys. **134**, 194506 (2011).
[14] G. R. Gathers, Int. J. Thermophys. **4**, 209 (1983).
[15] R. S. Hixson, M. A. Winkler, and M. L. Hodgdon, Phys. Rev. B **42**, 6485 (1990).
[16] H. Hess, E. Kaschnitz, and G. Pottlacher, High Press. Res. **12**, 29 (1994).
[17] M. H. Mousazadeh and M. G. Marageh, J. Phys.: Condens. Matter **18**, 4793 (2006).
[18] K. M. Watson, Ind. Eng. Chem. **35**, 398 (1943).
[19] D. S. Viswanath and N. R. Kuloor, J. Chem. Eng. Data **11**, 69 (1966).
[20] S. Velasco, F. L. Román, J. A. White, and A. Mulero, Fluid Phase Equilib. **244**, 11 (2006).
[21] E. A. Guggenheim, J. Chem. Phys. **13**, 253 (1945).
[22] A. Grossman, R. P. Doerner, and S. Luckhardt, J. Nucl. Mater. **290-293**, 80 (2001).
[23] D. Kashchiev, J. Chem. Phys. **118**, 1837 (2003).
[24] P. G. Debenedetti, *Metastable Liquids: Concepts and Principles* (Princeton University Press, Princeton, NJ, 1996).
[25] S. I. Anisimov, Sov. Phys. JETP **27**, 182 (1968).
[26] C. J. Knight, AIAA J. **17**, 519 (1979).
[27] W. Döring, Z. Phys. Chem. **36**, 371 (1937).
[28] M. Volmer, *Kinetik der Phasenbildung* (Steinkopff, Dresden, 1939).
[29] V. P. Skripov, *Metastable Liquids* (Wiley, New York, 1974).
[30] R. D. Torres, S. L. Johnson, R. F. Haglund, J. Hwang, P. L. Burn, and P. H. Holloway, Crit. Rev. Solid State Mater. Sci. **36**, 16 (2011).
[31] J. C. Alonso, R. Diamant, P. Castillo, M. C. Acosta-Garcia, N. Batina, and E. Haro-Poniatowski, Appl. Surf. Sci. **255**, 4933 (2009).
[32] C. Wu and L. V. Zhigilei, Appl. Phys. A **114**, 11 (2014).
[33] J. Hermann, S. Noël, T. E. Itina, E. Axente, and M. E. Povarnitsyn, Laser Phys. **18**, 374 (2008).